REPORT DOCUMENTATION PAGE

Form Approved
OMB No. 0704-0188

1. REPORT DATE *(DD-MM-YYYY)*	**2. REPORT TYPE**	**3. DATES COVERED** *(From - To)*
08-05-2008	Technical Paper	

4. TITLE AND SUBTITLE

Polynitrogen/Nanoaluminum Surface Interactions (Challenge Project C2V) (Preprint)

5a. CONTRACT NUMBER

5b. GRANT NUMBER

5c. PROGRAM ELEMENT NUMBER

6. AUTHOR(S)
Jerry A. Boatz (AFRL/RZSP); Dan C. Sorescu (DOE)

5d. PROJECT NUMBER
23030423

5e. TASK NUMBER

5f. WORK UNIT NUMBER

7. PERFORMING ORGANIZATION NAME(S) AND ADDRESS(ES)

Air Force Research Laboratory (AFMC)
AFRL/RZSP
10 E. Saturn Blvd.
Edwards AFB CA 93524-7680

8. PERFORMING ORGANIZATION REPORT NUMBER

AFRL-RZ-ED-TP-2008-182

9. SPONSORING / MONITORING AGENCY NAME(S) AND ADDRESS(ES)

Air Force Research Laboratory (AFMC)
AFRL/RZS
5 Pollux Drive
Edwards AFB CA 93524-70448

10. SPONSOR/MONITOR'S ACRONYM(S)

11. SPONSOR/MONITOR'S NUMBER(S)
AFRL-RZ-ED-TP-2008-182

12. DISTRIBUTION / AVAILABILITY STATEMENT

Approved for public release; distribution unlimited (PA #08208A).

13. SUPPLEMENTARY NOTES
For presentation at the DoD Users Group Conference, to be held in Seattle, WA, 14-17 July 2008.

14. ABSTRACT

First-principles density functional theory (DFT) calculations using the generalized gradient approximation (GGA) have been performed to study the adsorption of a series of all-nitrogen and high-nitrogen compounds of increasing sizes and complexity on the Al(111) surface. The calculations employ periodic slab models with 4 Al layers, ranging in size from (3x3) to (6x6) surface unit cells, and containing up to 144 Al atoms. Complementary quantum chemical calculations, utilizing DFT and second-order perturbation theory methods, of the ground state potential energy surfaces of the corresponding polynitrogen/high nitrogen species in the absence of the aluminum surface also have been performed. The initial set of studies performed in the first year of this challenge project, which focused on the adsorption and reaction properties of N_x (x=1-5), NH_x (x=1-3), N_2H_x (x=1-4), N_3H, N_3H_3 and N_4H_4 species on Al(111), have been extended to include larger polynitrogen systems such as N_6, N_8, N_{10} and N_{12}. The $C_{48}N_{12}$ fullerene-like molecule was included in this series in place of N_{60}, which was found to be unstable in the gas phase. Furthermore, simple nitrogen-containing heterocycles such as furazan ($C_2N_2H_2O$), 2H-1,2,3- and 4H-1,2,4-triazole ($C_2N_3H_3$), and 1H- and 2H-tetrazole (CN_4H_2) have been studied. Additional compounds of interest include the monosubstituted di(cyclopropyl)triazole ($C_{11}N_6H_{12}$) and di(cyclobutyl)triazole ($C_{13}N_5H_{16}$) derivatives of triazene. For these systems, surface interaction mechanisms involving both dissociative and nondissociative processes have been characterized as a function of molecular orientation and surface site. The dissociative mechanisms generally include elimination of one or more N_2 molecules.

15. SUBJECT TERMS

16. SECURITY CLASSIFICATION OF:			**17. LIMITATION OF ABSTRACT**	**18. NUMBER OF PAGES**	**19a. NAME OF RESPONSIBLE PERSON**
					Dr. Jerry A. Boatz
a. REPORT	**b. ABSTRACT**	**c. THIS PAGE**	SAR	8	**19b. TELEPHONE NUMBER** *(include area code)*
Unclassified	**Unclassified**	**Unclassified**			N/A

Polynitrogen/Nanoaluminum Surface Interactions (PREPRINT) (Challenge Project C2V)

Jerry A. Boatz, AFRL Propulsion Directorate, Space and Missile Propulsion Division, Edwards AFB, CA
(jerry.boatz@edwards.af.mil)
Dan C. Sorescu, US Department of Energy, National Energy Technology Laboratory, Pittsburgh, PA
(sorescu@netl.doe.gov)

ABSTRACT

First-principles density functional theory (DFT) calculations using the generalized gradient approximation (GGA) have been performed to study the adsorption of a series of all-nitrogen and high-nitrogen compounds of increasing sizes and complexity on the Al(111) surface. The calculations employ periodic slab models with 4 Al layers, ranging in size from (3x3) to (6x6) surface unit cells, and containing up to 144 Al atoms. Complementary quantum chemical calculations, utilizing DFT and second-order perturbation theory methods, of the ground state potential energy surfaces of the corresponding polynitrogen/high nitrogen species in the absence of the aluminum surface also have been performed. The initial set of studies performed in the first year of this challenge project, which focused on the adsorption and reaction properties of N_x (x=1-5), NH_x (x=1-3), N_2H_x (x=1-4), N_3H, N_3H_3 and N_4H_4 species on Al(111), have been extended to include larger polynitrogen systems such as N_6, N_8, N_{10} and N_{12}. The $C_{48}N_{12}$ fullerene-like molecule was included in this series in place of N_{60}, which was found to be unstable in the gas phase. Furthermore, simple nitrogen-containing heterocycles such as furazan ($C_2N_2H_2O$), 2H-1,2,3- and 4H-1,2,4-triazole ($C_2N_3H_3$), and 1H- and 2H-tetrazole (CN_4H_2) have been studied. Additional compounds of interest include the monosubstituted di(cyclopropyl)triazole ($C_{11}N_6H_{12}$) and di(cyclobutyl)triazole ($C_{13}N_5H_{16}$) derivatives of triazene. For these systems, surface interaction mechanisms involving both dissociative and nondissociative processes have been characterized as a function of molecular orientation and surface site. The dissociative mechanisms generally include elimination of one or more N_2 molecules.

I. Introduction

Investigation of the interactions of energetic high-nitrogen compounds with ultrafine or nanophase aluminum particles is a topic of current DoD interest with potential applications in rocket and missile propulsion. One of the topics of prime importance is to determine if the thermal instability inherent in many high nitrogen compounds might be reduced by adsorption or chemisorption onto the surface of aluminum, while simultaneously forming a protective coating on the metal surface which minimizes the formation of an inert oxide surface layer.

II. Computational Method

The calculations performed in this study were done using the Vienna *ab initio* simulation package (VASP).[1-3] This program evaluates the total energy of periodically repeating geometries based on density-functional theory and the pseudopotential approximation. In this case the electron-ion interaction is described by fully non-local optimized ultrasoft pseudopotentials similar to those introduced by Vanderbilt.[4,5] Periodic boundary conditions are used, with the one-electron pseudo-orbitals expanded over a plane-wave basis set. All calculations have been performed using a cutoff energy of 435 eV except for the furazan calculations. In this case, the energy cutoff was increased to 495 eV, due to the presence of O atom which requires a higher cutoff energy. These cutoff energies are consistent to the precision level high required by the pseudopotentials used by VASP code. Calculations were performed using the generalized gradient approximation (GGA) density functional theory with PW91 exchange-correlation functional.[6] The sampling of the Brillouin zone was performed using a Monkhorst-Pack scheme.[7] The minimum energy path between different minima was determined using the climbing image nudged elastic band method developed by Jónsson and co-workers.[8,9]

The GAMESS[10] quantum chemistry code was used to predict the structures and properties of isolated polynitrogen and high-nitrogen compounds. The theoretical methods employed included second order perturbation theory[11] (MP2, also known as MBPT(2)) and density functional theory (DFT) using the hybrid B3LYP[12] functional. The 6-311G(2df,p) basis set[13] was used throughout.

III. Results and Discussion

In our systematic analysis of high-nitrogen and polynitrogen compounds with the aluminum surface, we have considered a diverse number of chemical compounds in order to determine the adsorption and reaction properties of different chemical functionalities. The first set of compounds considered is the sequence of all-nitrogen molecules N_6, N_8, N_{10} and N_{12}, which extends the previous investigations of N_x (x=1-5) from the first year of this project. The $C_{48}N_{12}$ fullerene-like molecule was included in this series in place of N_{60}, which was found to be unstable in the gas phase. The second set of compounds considered in this study is comprised of simple nitrogen-containing heterocycles, including furazan ($C_2N_2H_2O$), 2H-1,2,3-triazole and 4H-1,2,4-triazole ($C_2N_3H_3$), and 1H- and 2H-tetrazole (CN_4H_2). The third set includes the monosubstituted di(cyclopropyl)triazole and di(cyclobutyl)triazole derivatives of triazene ($C_{11}N_6H_{12}$ and $C_{13}N_5H_{16}$, respectively.)

Due to the diversity in the size of the molecular systems analyzed in this study we have used in computations slab models of different sizes. These range from (3x3) surface supercells used in the case of small systems to (6x6) surface units for the largest systems. In all cases the slab models contained four layers of atoms. The optimizations have been performed for both the adsorbate and the Al atoms in the top two layers while the bottom two layers were frozen at the bulk optimized conditions. Adsorption at different surface sites and for different molecular orientations have been investigated and the corresponding adsorption energies have been calculated using the expression $\mathbf{E_{ads} = E_{molec} + E_{slab} - E_{(molec+slab)}}$, where E_{molec} is the energy of the isolated molecular species at its equilibrium geometry, E_{slab} is the total energy of the isolated aluminum slab, and $E_{(molec+slab)}$ is the total energy of the adsorbate/slab system. A positive E_{ads} corresponds to a thermodynamically stable adsorbate/slab system. In the present study, only neutral species have been considered.

N_x (x=6, 8, 10, 12) Adsorption on Al(111). The adsorption properties of N_x (x=6, 8, 10, 12) have been characterized using a (3x3) supercell aluminum slab model for N_6 and N_8, and a (4x4) slab model for N_{10} and N_{12}. Representative adsorption configurations are presented in Figures 1a-1l. In the case of N_6, both an open-chain (C_{2h}) and a cyclic (D_2) isomer have been considered. Similarly, for N_8 both the azidopentazole (C_s) and octaazapentalene (D_{2h}) isomers have been investigated. Upon optimization, the open-chain N_6 isomer was found to dissociate to form two N_3 species which bind on the surface in either horizontal or vertical orientations, as illustrated in Figure 1a. In contrast, the cyclic N_6 isomer molecularly adsorbs on the surface with formation of multiple Al-N bonds, as shown in Figure 1b. For cyclic N_6, the binding energies range from 49.3 to 64.8 kcal/mol, relative to the isolated slab and gas phase N_6 molecule. In the case of N_8, both the azidopentazole (Figures 1c-1e) and octaazapentalene (Figure 1f) were found to adsorb molecularly. For azidopentazole, significant variations in binding energies, ranging from 10.5 to 63.1 kcal/mol, were found as a function of specific molecular orientation and the number of Al-N bonds formed (see Figures 1c-1e.) In some instances, azidopentazole was found to dissociate on the surface, leading to formation of adsorbed N_5+N_3 or N_6+N_2 fragment pairs. All of these reactive processes are exothermic with respect to the undissociated configurations (see Figures 1c-1d.) Likewise, dissociation of octaazapentalene to N_5 + N_3 (Figure 1f) is exothermic by about 64 kcal/mol. Similar reaction processes were also observed for the N_{10} molecule. For example, N_{10} can adsorb without undergoing fragmentation (Figure 1g) or by a dissociative process in which one of the molecular rings is broken with subsequent formation of multiple Al-N bonds (Figure 1h.) Additional dissociative mechanisms include the formation of two adsorbed N_5 species (Figure 1i) or an adsorbed N_6 fragment plus two N_2 molecules which readily desorb (Figure 1j). The dissociative adsorption mechanisms of N_{10} were found to be highly exothermic, with dissociation enthalpies as high as 101 kcal/mol relative to the adsorbed, undissociated state. Finally, in the case of the N_{12} system, molecular adsorption was found to be possible with binding energies in the range 55.5-60.4 kcal/mol (see Figures 1k-1l.) The presence of several Al-N bonds in this case contributes to the increased stability of this molecular system.

By comparing the current set of results to the prior adsorption data for N_x (x=1,5), it can be concluded that adsorbed N atoms are the most stable species. Additionally, for the larger systems analyzed here, the surface dissociation leading to formation of N, N_2, N_3 fragments is highly exothermic. Not surprisingly, the interaction of N_2 with the Al surface is weak, leading to facile desorption.

Adsorption of $C_{48}N_{12}$ Fullerene-like Systems. Three distinct configurations of the $C_{48}N_{12}$ fullerene-like cage on the Al surface have been identified. The most stable structure, with a binding energy of 12 kcal/mol, is obtained by the attachment of the $C_{48}N_{12}$ cage to the Al surface via adjacent carbon atoms, as shown in Figure 1n. The configuration in which the fullerene cage is attached to the Al surface via a pair of neighboring carbon and nitrogen atoms (Figure 1o) is somewhat less stable, with a binding energy of 10.9 kcal/mol. The least stable structure, shown

in Figure 1p, involves binding of the fullerene cage to the surface via two non-adjacent carbon atoms, with a binding energy of 4.5 kcal/mol. No dissociative adsorption pathways were observed for $C_{48}N_{12}$ on the Al surface.

Furazan Adsorption and Dissociation on Al(111). Adsorption of the furazan ring on the Al surface can occur in vertical or horizontal configurations as illustrated in Figures 2a-2d, with a preference for the vertical state (Figure 2a), which has a modest binding energy of 7.3 kcal/mol. The adsorbed furazan ring can readily dissociate on the surface with a large amount of energy released. This is illustrated in Figures 2m-2n which show the minimum energy pathways for molecular dissociation on the surface starting from an initial horizontal local minimum (Figure 2m) and from an initial vertical configuration (Figure 2n.) As indicated in these figures, the corresponding activation energies for molecular dissociation are very small but the overall reactions are highly exothermic; e.g., 187 kcal/mol starting from the horizontal configuration.

Adsorption of 2H-1,2,3-triazole, 4H-1,2,4-triazole, 1H-tetrazole, and 2H-tetrazole. Illustrative examples of the adsorption configurations of 2H-1,2,3-triazole, 4H-1,2,4-triazole, 1H-tetrazole, and 2H-tetrazole are indicated in Figures 2e-2l. The corresponding binding energies are moderate, with values of 10.8, 15.7, 10.7, and 8.0 kcal/mol, respectively. In all cases, a vertical orientation of the ring and attachment to the surface via one or two nitrogen atoms is the preferred adsorption configuration.

Adsorption of mono-substituted triazenes. As an extension of our previous results on the aluminum surface adsorption of the 1,3,5- and 1,2,3-triazene molecules, the surface interactions of the monosubstituted di(cyclobutyl)triazole ($C_{13}H_{16}N_6$) and di(cyclopropyl)triazole ($C_{11}H_{12}N_6$) derivatives of triazene have been investigated. These calculations have been performed using a (5x5) surface slab model. Figure 3 illustrates the results for these two systems, which shows four adsorption configurations for the cyclobutyl (Figures 3a-3d) and cyclopropyl (Figures 3e-3g) derivatives. In all cases, the cycloalkyl groups do not bind to the aluminum surface. The most stable configurations of the cyclobutyl (Figure 3a) and cyclopropyl (Figure 3e) systems involve binding to the surface via the formation of multiple bonds between aluminum and the 6-membered triazene moiety plus an additional Al-N bond to a nitrogen atom of the triazole substituent, with binding energies of 25.1 and 21.6 kcal.mol, respectively. A similar but less stable configuration for the cyclobutyl derivative was found in which there is no bond between an aluminum atom and the triazole moiety (Figure 3b.) Additional configurations in which bonding to the surface occurs via a single nitrogen atom of the triazene ring are also possible, as shown in Figures 3d and 3f, with respective binding energies of 12.3 and 12.5 kcal/mol. The least stable configurations show a horizontal orientation of the triazene moiety, as illustrated in Figures 3c, 3g, and 3h. The latter two structures show that a significant portion of the stabilization energy gained from formation of Al-N or Al-C bonds can be lost in the deformation of the gas phase structure and/or in the upward movement of some of the surface Al atoms. This is the case for the structures depicted in Figures 3g and 3h, which both have negative binding energies despite the fact that a number of Al-N and Al-C bonds have been formed. In the present sign convention, the negative binding energies indicate that these structures are thermodynamically unstable relative to the isolated gas phase molecule and the isolated surface.

IV. Conclusions

A systematic study of a series of polynitrogen and high nitrogen species (N_x; x=6,8,10,12, the $C_{48}N_{12}$ fullerene analogue, simple nitrogen-containing heterocycles such as furazan, triazole, and tetrazole, and monosubstituted di(cycloalkyl)triazole derivatives of triazene) interacting with the aluminum (111) surface have been investigated using plane-wave DFT calculations in conjunction with aluminum surface slab models. Our calculations indicate that, in the majority of cases molecular adsorption takes place by formation of multiple Al-N or Al-C bonds. For the ensemble of molecular systems considered here, a significant range of variation in binding energies has been determined depending on the number of surface bonds involved as well as the surface site and the molecular orientation. Additionally, the adsorption was found to lead to important molecular deformations and to upward shifts of some of the surface aluminum atoms. For the all-nitrogen species, dissociative adsorption readily occurs, particularly for the N_6-N_{10} species, with a large energy release. Dissociation often leads to desorption of N_2 species and/or deposition of N atoms. The overall dissociation processes were found to be exothermic. Such findings were also found for furazan, where molecular dissociation takes place with a large amount of energy release.

Future work will extend this set of investigations to include additional high-nitrogen and polynitrogen systems such as 3,3'-azobis(6-amino-1,2,4,5-tetrazine) ($C_4N_{12}H_4$) as well as a systematic analysis of the thermal

effects on the adsorption and reaction processes.

Acknowledgements

The authors gratefully acknowledge grants of computer time at the Air Force Research Laboratory, Engineer Research and Development Center, and the Naval Oceanographic Office Major Shared Resource Centers, sponsored by the Department of Defense High Performance Computing Modernization Program.

References

1. Kresse, G.; Hafner, J. *Phys. Rev*. **1993**, B 48, 13115.
2. Kresse, G. ; Furthmüller, J. *Comput. Mat. Sci*. **1996**, 6, 15.
3. Kresse, G.; Furthmüller, J. *Phys. Rev*. **1996**, B 54, 11169.
4. Vanderbilt, D. *Phys. Rev*. **1990**, B 41, 7892.
5. Kresse, G; Hafner, J. *J. Phys. Condens. Matter* **1994**, 6, 824.
6. Perdew, J. P.; Chevary, J. A.; Vosko, S. H.; Jackson, K. A.; Pedersen, M. R.; Singh, D. J.; Frolhais, C. *Phys. Rev*. **1992**, B 46, 6671.
7. Monkhorst, H. J.; Pack, J. D. *Phys. Rev*. **1976**, B 13, 5188.
8. Jónsson, H.; Mills, G. Jacobsen, K. W. *Nudged elastic band method for finding minimum energy paths of transitions*. In C*lassical Quantum Dynamics in Condensed Phase Simulations*; Berne, B. J., Ciccotti, G., Coker, D. F., Eds.; World Scientific: Singapore. 1998; p 385.
9. Henkelman, G.; Uberuaga, B. P.; Jónsson, H. *J. Chem. Phys.* **2000**, 113, 9901.
10. a) Schmidt, M.W.; Baldridge, K.K.; Boatz, J.A.; Elbert, S.T.; Gordon, M.S.; Jensen, J.H.; Koseki, S.; Matsunaga, N.; Nguyen, K.A.; Su, S.J.; Windus, T.L.; Dupuis, M.; Montgomery, J.A. *J.Comput.Chem*. **1993**, 14, 1347.
    b) Gordon, M.S.; Schmidt, M.W. in "Theory and Applications of Computational Chemistry, the first forty years" C.E.Dykstra, G.Frenking, K.S.Kim, G.E.Scuseria, Elsevier, Amsterdam, 2005.
11. a) Moller, C. ; Plesset, M.S. ; *Phys. Rev*. **1934,** *46*, 618.
    b) Pople, J.A.; Binkley, J.S.; Seeger, R. *Int. J. Quantum Chem. S10*, **1976**, 1.
    c) Frisch, M.J.; Head-Gordon, M.; Pople, J.A. *Chem.Phys.Lett.* **1990**, *166*, 275.
    d) Bartlett, R.J; Silver, D.M. *Int. J. Quantum Chem. Symp.* **1975,** *9*, 1927.
12. a) Becke, A.D.; *J. Chem. Phys*. **1993**, *98*, 5648.
    b) Stephens, P.J.; Devlin, F.J.; Chablowski, C.F.; Frisch, M.J. *J. Phys. Chem*. **1994,** 98, 11623.
    c) Hertwig, R.H.; Koch, W. *Chem. Phys. Lett*. **1997**, 268, 345.
    d) Vosko, S.H.; Wilk, L.; Nusair, M. *Can. J. Phys.* **1980**, 58, 1200.
13. a) Krishnan, R.; Binkley, J.S.; Seeger, R.; Pople, J.A. *J.Chem.Phys*. **1980**, 72, 650.
    b)Frisch, M.J.; Pople, J.A.; Binkley, J.S. *J. Chem. Phys*. **1984**, 80, 3265.

Figure Captions

Figure 1. Side and top views of the most stable adsorption configurations of (a) N_6 (open-chain) and (b) N_6 (cyclic) molecules. Side views of N_8-azidopentazole (c)-(e), N_8-octaazapentalene (f), N_{10} (g)-(j), and N_{12} (k)-(l) on the Al(111) surface. Panel (m) illustrates the gas phase structure of the $C_{48}N_{12}$ molecule. Adsorption configurations involving adjacent carbon atoms, adjacent carbon and nitrogen atoms, or nonadjacent carbon atoms in $C_{48}N_{12}$ are shown in panels (n)-(p), respectively.

Figure 2. Side views of representative binding configurations of furazan (a-d), 2H-1,2,3-triazole (e,f), 4H-1,2,4-triazole (g,h), 1H-tetrazole (i,j), and 2H-tetrazole (k,l). Panels (m) and (n) indicate the minimum energy pathways for furazan dissociation starting from horizontal and vertical adsorption configurations, respectively.

Figure 3. Representative adsorption configurations of the monosubstituted di(cyclobutyl)triazole (a-d) and di(cyclopropyl)triazole (e-h) triazene derivatives and the corresponding binding energies.

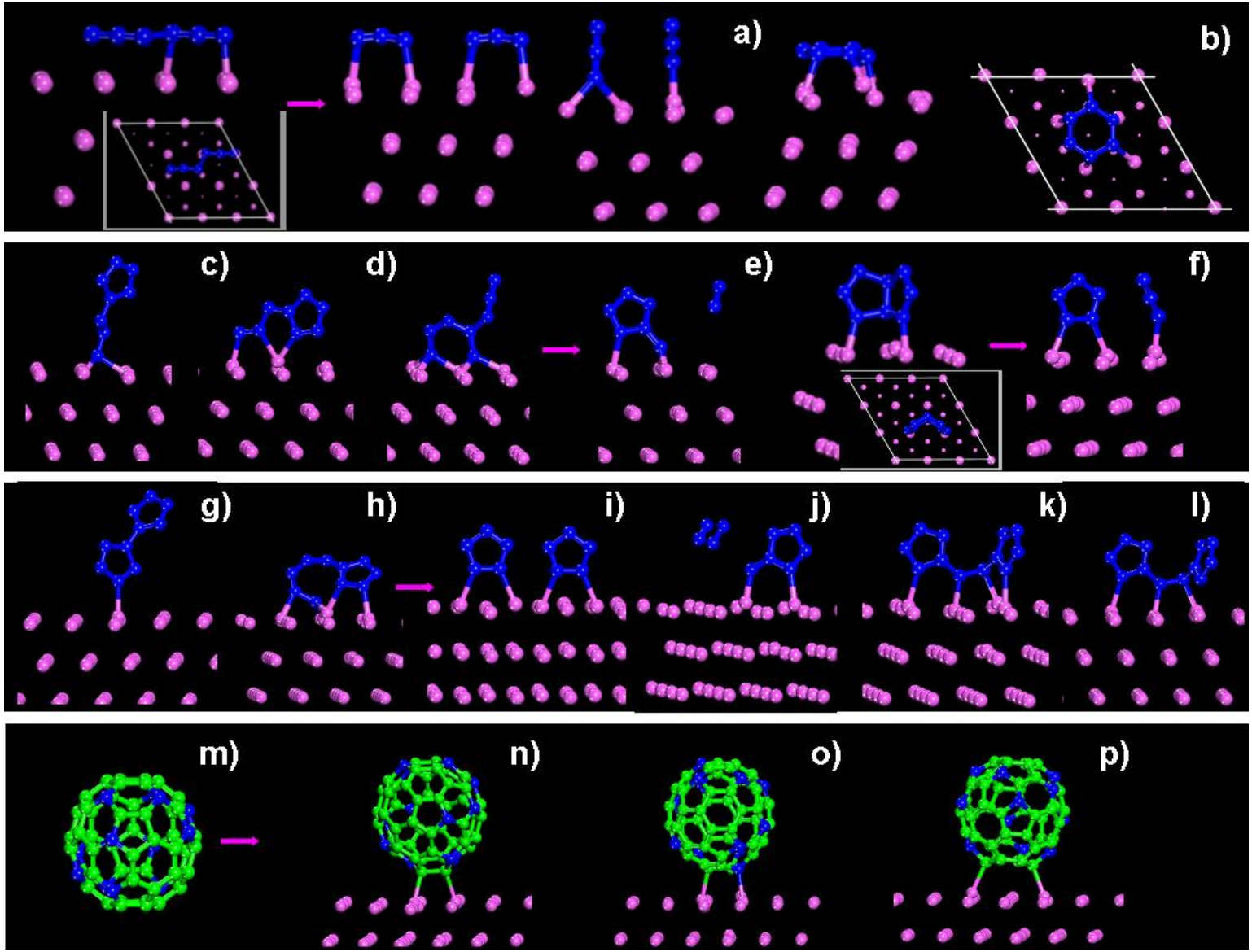

Figure 1

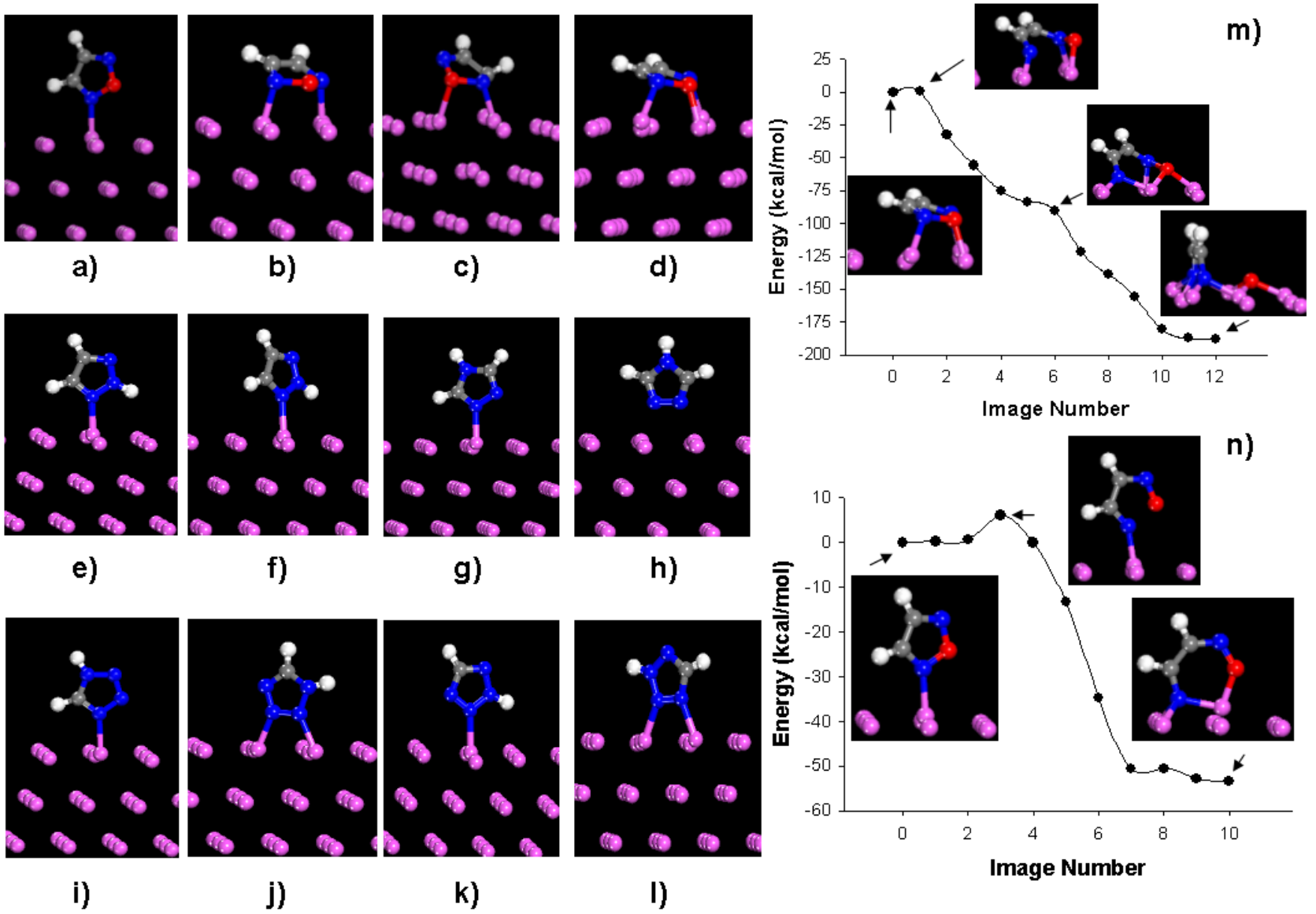
a)
b)
c)
d)
e)
f)
g)
h)
i)
j)
k)
l)
m)
Energy (kcal/mol)
25
0
-25
-50
-75
-100
-125
-150
-175
-200
0
2
4
6
8
10
12
Image Number
n)
Energy (kcal/mol)
10
0
-10
-20
-30
-40
-50
-60
0
2
4
6
8
10
Image Number

Figure 2

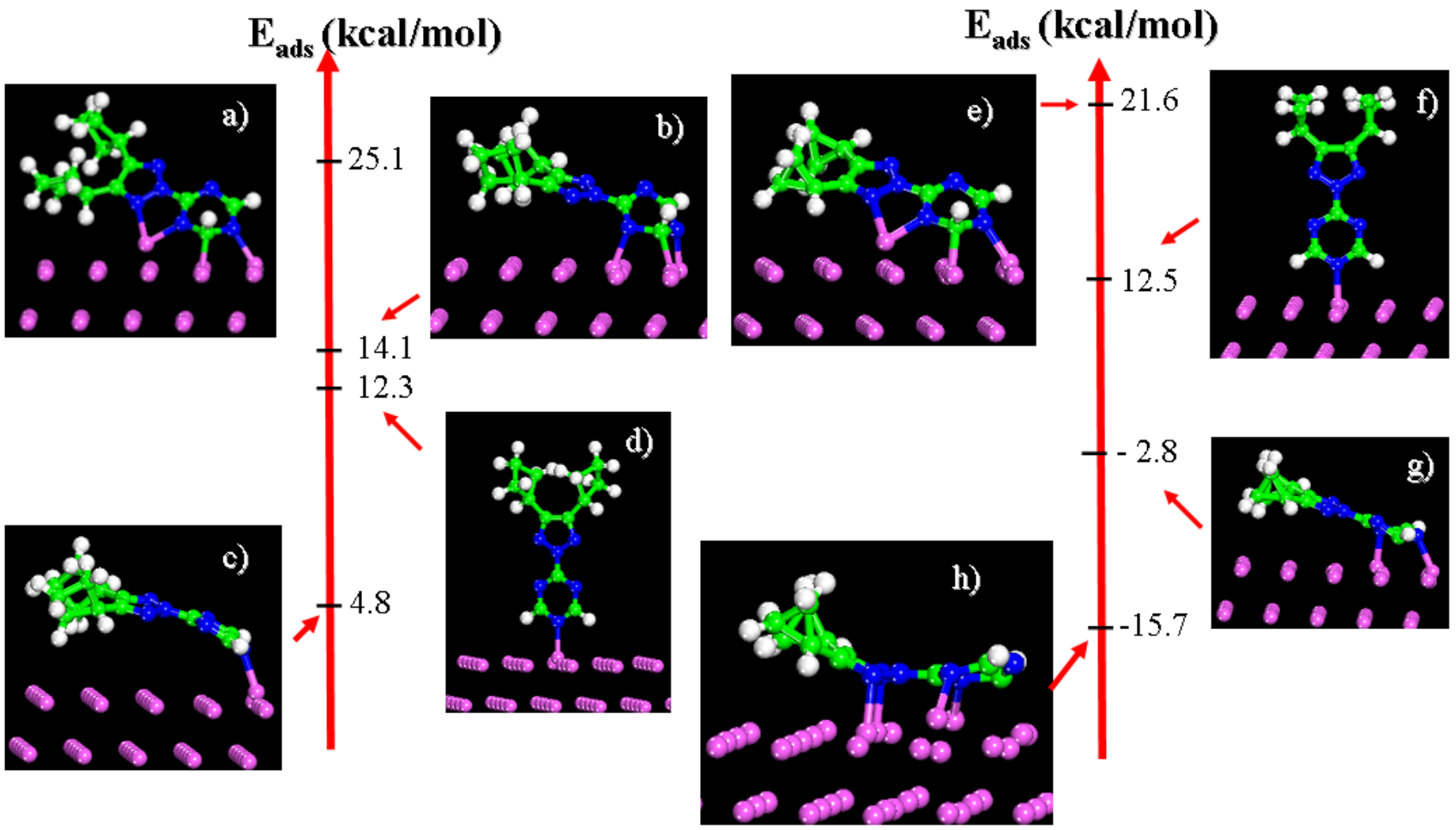
E_ads (kcal/mol)
a)
b)
c)
d)
e)
f)
g)
h)
25.1
14.1
12.3
4.8
E_ads (kcal/mol)
21.6
12.5
- 2.8
-15.7

Figure 3